Thermally Stimulated Currents in Semiconductors and Insulators Having Arbitrary Trap Distributions*

J. G. Simmons, G. W. Taylor, and M. C. Tam†
Electrical Engineering Department, University of Toronto, Toronto, Canada
(Received 2 June 1972)

The theory is developed for thermally stimulated currents (TSC) that flow in optically or electrically excited insulators and semiconductors in which the field is sufficiently high and the (active) region in which the free carriers are generated is sufficiently thin (e.g., reverse-biased junctions, thin films, etc.) so that recombination rate of the free carriers is negligible. Closed-form solutions are obtained for the TSC characteristics for semiconductors and insulators containing *arbitrary* trap distributions. Using various *ad hoc* trapping distributions, it is shown that the approximate high-field TSC characteristics correlate extremely well with the exact characteristics that were computed numerically. More important, however, it is shown that the *shape* of the observed TSC characteristic is a *direct* reflection of the sum of the trap distribution in the upper half and the lower half of the band gap. The technique is potentially a powerful means of characterizing trap distributions in defect semiconductors and insulators, in that it permits the direct determination of the trap distribution without requiring an *a priori* knowledge of the trap parameters and without the need for laborious analyses.

I. INTRODUCTION

The thermally-stimulated-current (TSC) technique is, in principle, a useful method for studying the defect nature of semiconductors and insulators.[1-6] However, the theory of TSC has been developed for only a few very simple, *ad hoc* cases involving discrete trap levels. A general treatment of the problem involving traps that are *arbitrarily distributed* throughout the band gap appears to be intractable to analytical solution. This is rather unfortunate, since distributed traps are commonly found in a wide range of insulators and semiconductors, particularly those existing in polycrystalline and amorphous forms. Even for the simple cases that have been theoretically analyzed, it is noted that because of the intractability of the pertinent theoretical equations and the number and uncertainty of the physical parameters involved it is extremely difficult to correlate theory with experiment. In fact, Kelly and Braunlich[7] have noted that TSC (and thermally luminescent) experiments do not yield sufficient information to determine the kinetic mechanism of the thermally stimulated recombination process without *a priori* knowledge of most of the trapping parameters.

Putting the above-mentioned limitations aside, we believe that problems still exist, in that parts of the theoretical formulation are suspect because they are based on single-carrier (electron) kinetics, yet the problem is clearly a two-carrier problem. It does not suffice to effectively eliminate hole kinetics from consideration simply by assuming that once generated the hole is immediately trapped and effectively removed from the conduction process. The existence of free holes in non-steady-state processes, such as TSC, or steady-state processes,[8] is just as indispensable as that of electrons in determining the recombination-generation processes and the statistics of occupation of the traps.

In a recent paper[9] we showed that many of the above-mentioned problems could be effectively eliminated and the problem formulated accurately by applying a high field to a thin (active) region of the material so that the generated electrons and holes can be removed from the active region before they can recombine. This technique, which we designated the *high-field* TSC process,[9,10] is readily applicable to a wide range of problems, including reverse-biased p-n junctions, Shottky barriers, metal-insulator-semiconductor systems, and thin insulating and semiconducting films. The object of this paper is to extend the treatment of high-field TSC to that of systems containing arbitrary trap distributions. Apart from the fact that the problem can be solved in closed form, we will show that the shape of the TSC characteristic is a *direct image* of the energy distribution of traps.

In order to keep the paper concise, we will assume that the reader is familiar with Paper I[10] and the earlier paper on high-field TSC,[9] so that we do not have to go into a detailed discussion of the high-field concepts and the parameters used in formulating the problem. Also, as in Paper I, we will assume in the formulation of the problem that the traps have been optically excited, but it should be borne in mind that the theory is, in fact, applicable to electrically excited traps.[11-13]

II. THEORY

Suppose that a solid containing traps has been radiated with light at a low temperature and after the

light is removed, a high field is applied to the solid. The relaxation electron and hole currents as a function of time t and temperature T are given in Ref. 10 by Eqs. (3) and (4), respectively. Now, let the temperature be raised at a constant rate so that the following explicit relationship exists between temperature and time:

$$T = \beta t + T_0, \tag{1}$$

where β is the heating rate and T_0 is the low temperature at which the solid was irradiated with light. Substituting our Eq. (1) into Eqs. (3) and (4) of Ref. 11 yields

$$I_n = \tfrac{1}{2} qL \int_{E_i}^{E_c} f_0(E) N(E) e_n(E, T) \times \exp\left(-\frac{1}{\beta}\int_{T_0}^{T} e_n(E, T)\, dT\right) dE \tag{2}$$

and

$$I_p = \tfrac{1}{2} qL \int_{E_v}^{E_i} [1 - f_0(E)] N(E) e_p(E, T) \times \exp\left(-\frac{1}{\beta}\int_{T_0}^{T} e_p(E, T)\, dT\right) dE\,. \tag{3}$$

The total current I flowing in the system is, of course, given by

$$I = I_n + I_p. \tag{4}$$

Generally speaking, it is not possible to solve (2) and (3) for an *arbitrary* trap distribution $N(E)$. However, by a judicious examination of the integrand, we will show that (2) and (3) may be solved in approximate form to a high degree of accuracy.

A. High-Field TSC Characteristic

Consider the function $P(E, T)$ defined by

$$P(E, T) = e_n(E, T) \exp\left(-\frac{1}{\beta}\int_{T_0}^{T} e_n(E, T)\, dT\right) \tag{5}$$

that appears in the integrand of (2). This function is plotted as a function of energy for several different temperatures in Fig. 1, and it is seen to exhibit a pronounced narrow peak that has a halfwidth of approximately $2kT$ about the energy E_{mn} at which the maximum in $P(E, T)$ occurs. Physically speaking, this means that it is those traps positioned within an energy $2kT$ of E_{mn} that contribute most significantly to the current. From Fig. 1 it is apparent that E_{mn} moves away from the bottom of the conduction band with increasing temperature.

The relationship between E_{mn} and T may be obtained by differentiating $P(E, T)$ with respect to E and equating the derivative to zero:

$$\left.\frac{\partial P(E, T)}{\partial E_n}\right|_{E = E_{mn}} = 0, \tag{6}$$

which, from (5), yields

$$\frac{T}{\beta}\int_{T_0}^{T} \frac{e_n(E_{mn}, T)}{T}\, dT = 1. \tag{7}$$

For $E_c - E_{mn} \gg kT$, which will normally be the case, we have (see Appendix A)

$$kT^2 e_n(E_{mn}T)/\beta(E_c - E_{mn}) = 1. \tag{8}$$

Equation (8) is a transcendental function in E_{mn} and T that may be expressed in the more convenient analytical form[9]:

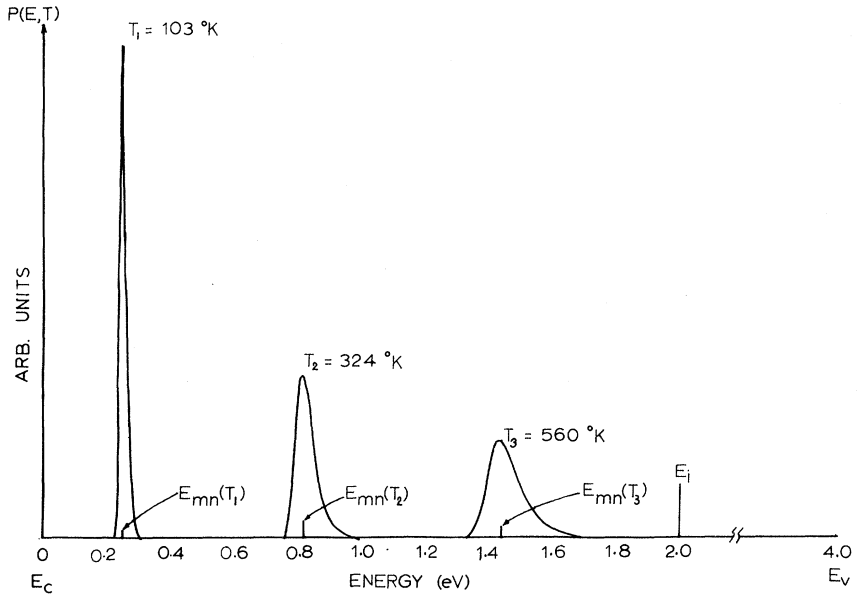

FIG. 1. Variation of $P(E, T)$ with temperature.

$$E_c - E_{mn} = T(1.92\times10^{-4}\log_{10}\frac{\nu}{\beta} + 3.2\times10^{-4}) - 0.015. \quad (9)$$

It is evident from Fig. 1 that $P(E, T)$ can be approximated by the δ function $\delta(E - E_{mn})$:

$$D\delta(E - E_m) = e_n(E, T)\exp\left(-\frac{1}{\beta}\int_{T_0}^{T} e_n(E, T)\,dT\right). \quad (10)$$

In (10), D is the area associated with the δ function and is evaluated by integrating both sides of (10):

$$D = \int_{E_v}^{E_c} e_n(E, T)\exp\left(-\frac{1}{\beta}\int_{T_0}^{T} e_n(E, T)dT\right)dE, \quad (11)$$

which yields [see (A10) of Appendix A]

$$D = 1.2\,\beta(E_c - E_{mn})/T. \quad (12)$$

[An inspection of (9) and (12) shows that D is only very slightly temperature dependent.] Substituting (10) into (2) yields

$$I_n = \tfrac{1}{2}qL\int_{E_t}^{E_c} f_0(E)N(E)\,D\,\delta(E - E_{mn})\,dE, \quad (13)$$

which integrates to

$$I_n = \tfrac{1}{2}qLDf_0(E)\,N(E_{mn}). \quad (14)$$

Using the same procedure as that leading to (14), one can readily show that the high-field TSC hole current is given by

$$I_p = \tfrac{1}{2}qLD[\,1 - f_0(E)]\,N(E_{mp}). \quad (15)$$

In (15), E_{mp} is the energy around which are positioned the hole traps that contribute most to the hole current:

$$E_{mp} - E_v = T(1.92\times10^{-4}\log_{10}\frac{\nu}{\beta} + 3.2\times10^{-4}) - 0.0155. \quad (16)$$

B. Relationship between High-Field TSC Characteristic and Trapping Distribution

Equation (14) states that the high-field TSC at a given temperature T is directly proportional to the density of the occupied traps $f_0(E)\,N(E_{mn})$ at E_{mn}. Thus, plotting the TSC characteristic as a function of temperature and then converting the temperature scale to an energy scale, using (9), provides a *direct* image of the *occupied* trap distribution in the upper half of the band gap between E_{tn} and E_i, that is, the initially occupied electron-emitting trap levels. When the ratio of the electron to hole-trap-capture cross sections is constant, f_o is constant,[8] a condition we will assume throughout the rest of this paper. In this event, it will be apparent that the TSC characteristic is a direct reflection of the trap distribution between E_{tn} and E_i.

In order to demonstrate the accuracy of the approximation used and, hence, to show that the actual TSC characteristic is indeed a direct image of the trap distribution, we proceed as follows: Consider the bimodal distribution shown by the full curve in the upper half of the band gap in Fig. 2(a). According to (14), this curve is also a good approximation to the stimulated-electron characteristic associated with the distribution in the energy range $E_{tn} - E_i$ when the energy axis is transformed into a temperature axis using (9) and the trap distribution scaled by the factor $qLDf_0\frac{1}{2}(E)$, as shown in Fig. 2(a). The *exact* electronic TSC current has also been calculated numerically using (2), and the resulting characteristic is shown by the dotted curve in the energy range E_{tn} to E_i in Fig. 2(a). The excellent correlation between the two sets of characteristics show that: (i) the approximations used here are extremely good, and (ii) the actual TSC characteristic is indeed a direct image of the trap distribution.

Applying similar arguments to (15) and (16), it follows that the thermally stimulated I_p vs T characteristic associated with hole-emitting traps will be a direct image of the trap distribution between the energies E_{tp} and E_i in the lower half of the band gap, as illustrated in Fig. 2(a).

Since the observed *high-field* current I is the *sum* of the electron current and the hole current, it follows that structure in the observed high-field TSC characteristic reflects the *sum* of the trap distribution between E_{tn} and E_i and between E_{tp} and E_i as indicated in Fig. 2(b). Clearly, then, the trapping distribution is not uniquely determined from the observed high-field TSC characteristic since it is not apparent whether the various portions of the characteristic reflect the trapping distribution in the upper half or lower-half of the band gap. Hall measurements made simultaneously with the TSC measurements would presumably provide the means for identifying whether the various parts of the TSC characteristic are to be associated with electron-emitting traps or hole-emitting traps. As previously mentioned in Paper I, the same ambiguity exists in identifying the *low-field* TSC characteristic with the position of the traps in the band gap (although, generally speaking, this point tends to be glossed over).

The curves marked A and B in Fig. 3 are the approximate (14) and exact (2) high-field TSC characteristics for a trap distribution that is constant in the energy range 0.5 – 1.25 eV below the bottom of the conduction band. Although this distribution is unlikely to be met with in practice, it is presented because it provides the most stringent test of the concepts presented here. It is seen that the approximate and exact high-field TSC curves correlate reasonably well, and that certainly the trap distribution is reflected quite well in the exact characteristic. The correlation between the shape of the observed high-field TSC curves and the ac-

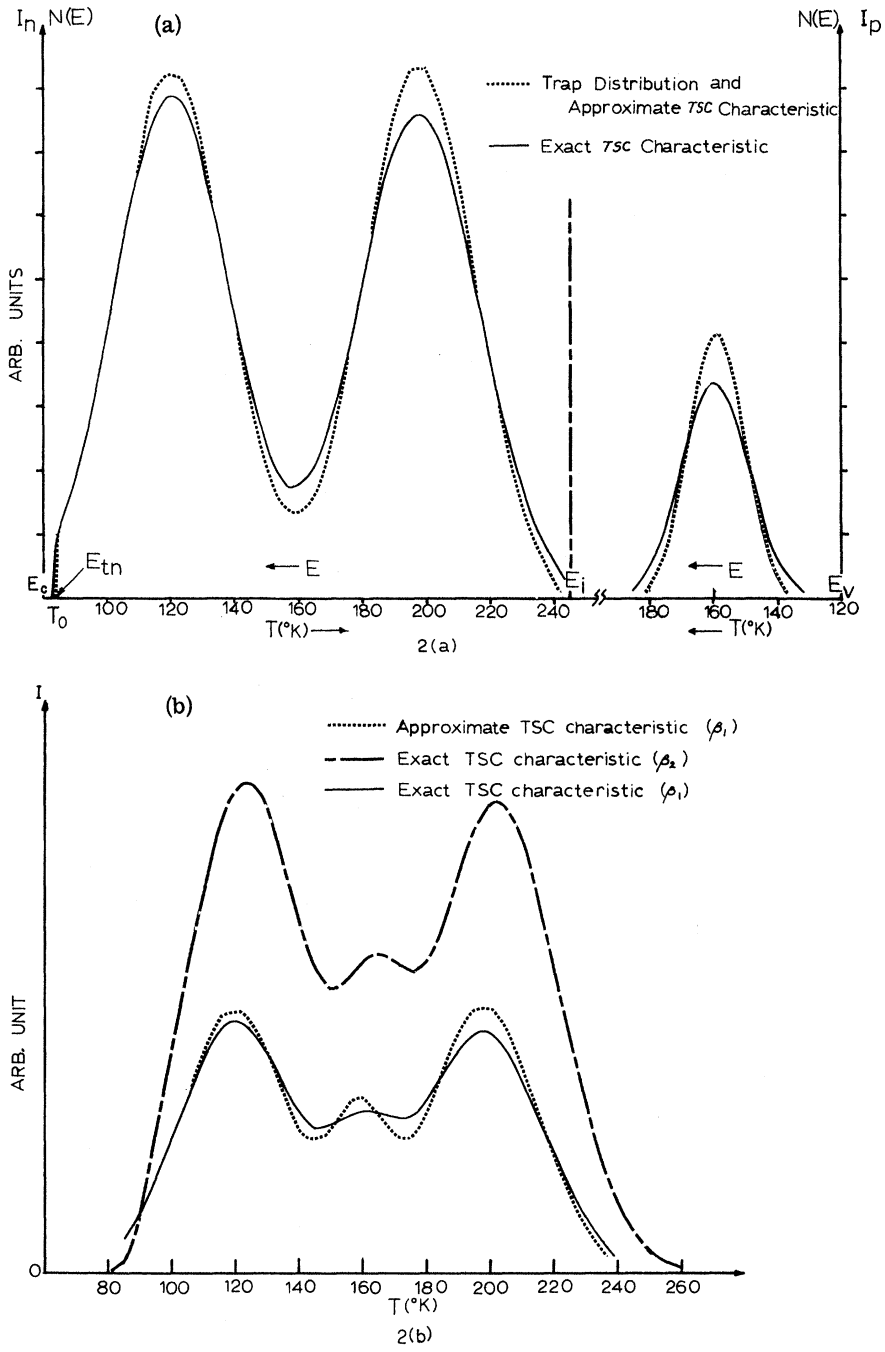

FIG. 2. (a) Trapping distribution $N(E)$ and approximate and exact electron and hole high-field TSC characteristics. (b) Observable approximate and high-field TSC characteristic associated with trapping distribution shown in (a). The actual characteristic is shown for two different heating rates.

tual trap distribution deteriorates for trap distributions less than about $4kT$ wide. Such distributions are best discussed in terms of the discrete trap-distribution concepts described in an earlier paper.[9]

Increasing the heating rate β causes a shift in the TSC characteristic to higher temperatures, as shown in Fig. 2(b). It will also be noted that the current scales almost linearly with β.

C. Attempt-to-Escape Frequency

The attempt-to-escape frequency ν is usually of the order of 10^{10} to 10^{12} sec^{-1}, and is conceivably different for electron-emitting traps and hole-emitting traps. Its value may be ascertained by measuring the TSC at two different heating rates, say β_1 and β_2, and by measuring the temperatures T_1 and T_2 at which a prominent part of the char-

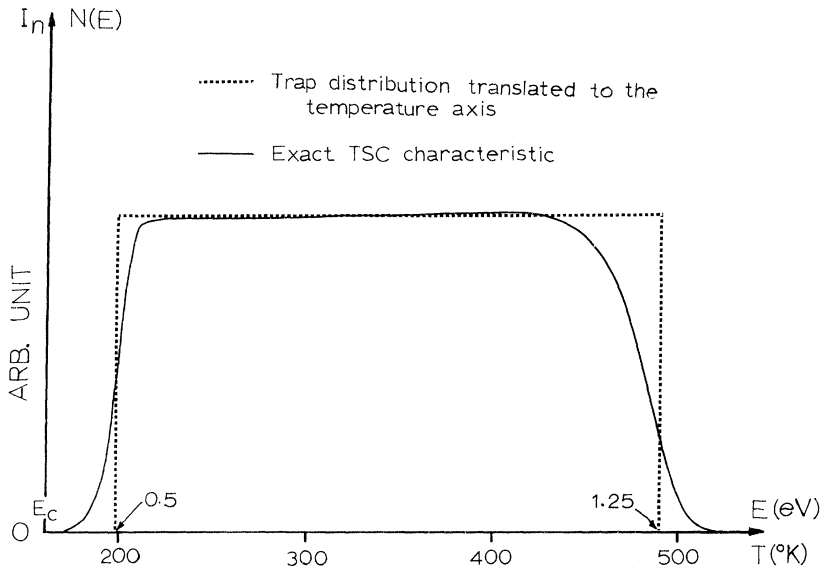

FIG. 3. Exact and approximate high-field TSC characteristics for a trap distribution that is constant in the energy range 0.5–1.25 eV below the bottom of the conduction band.

acteristic, corresponding to an energy ΔE measured with respect to either the valence- or conduction-band edge, appears. Hence, from (9), ν is determined from the expression

$$\nu = 10^{y}, \tag{17}$$

where

$$y = [(T_2 \log_{10} \beta_2 - T_1 \log_{10} \beta_1)/(T_2 - T_1)] - 1.66. \tag{18}$$

The energy dependence of ν, if any, may be determined by repeating the above procedure on matching points, corresponding to various energies of the pair of TSC characteristics.

III. CONCLUSIONS

We have presented approximate closed-form solutions for the high-field TSC characteristics for materials containing arbitrary distributions of traps throughout their band gaps. It has been shown that the solutions are an extremely good approximation to the exact characteristics, which were computed numerically. More important, however, it has been demonstrated that the shape of the TSC characteristics are a direct image of the trap distribution, and, as such, provide a valuable mean of investigating the defect nature of materials. There are, however, certain problems associated with the technique, in that it is not possible to determine unambiguously from the high-field TSC characteristic *per se* whether the various portions of the characteristic are to be identified with electron-emitting traps or hole-emitting traps, although Hall measurements carried out simultaneously with the high-field TSC measurement should assist in clarifying this point.

APPENDIX A

The integral

$$I = \frac{T}{\beta}\int_{T_0}^{T} \frac{e_n(E_{mn}T)}{T}\,dT \tag{A1}$$

may be integrated by parts to yield

$$I = \frac{T}{\beta}\left[\frac{kT\,e_n}{(E_c - E_{mn})} - \int_{T_0}^{T} \frac{k}{\Delta E}\,e_n\,dT\right]. \tag{A2}$$

The second integral on the right-hand side of (A5) may be evaluated[9] approximately to yield

$$\int_{T_0}^{T} \frac{k}{\Delta E}\,e_n\,dT = \left(\frac{kT}{E_c - E_{mn}}\right)^2 e_n(E_{mn}, T). \tag{A3}$$

Since $kT \ll E_c - E_t$ for typical parameter values, then the second term on the right-hand side of (A2) is small compared to the first term, thus

$$\frac{T}{\beta}\int_{T_0}^{T} \frac{e_n(E_{mn}, T)}{T}\,dT = \frac{kTe_n(E_{mn}, T)}{\beta(E_c - E_{mn})}. \tag{A4}$$

APPENDIX B

In Ref. 9 it was shown that

$$\exp\left(-\frac{1}{\beta}\int_{T_0}^{T} e_n(E, T)\,dT\right) \simeq [1 + 1.7\,e^{2(E - E_{mn})/kT}]^{-1}. \tag{A5}$$

Substituting (A5) into (11) yields

$$D = \int_{E_v}^{E_c} \frac{e_n(E, T)dE}{1 + 1.7\,e^{2(E - E_{mn})/kT}}. \tag{A6}$$

Using $x = e^{(E - E_c)/kT}$ in (A6) yields

$$D = -kT\nu\int_{e^{(E_v - E_c)/kT}}^{1} \frac{dx}{1 + bx^2}, \tag{A7}$$

where $b = 1.7e^{(E_{mn}-E_c)/kT}$. Integrating (A7) yields

$$D = \frac{kT\nu}{1.7} e^{(E_{mn}-E_c)/kT}\left[\tan^{-1}(1.7e^{(E_{mn}-E_v)/kT}) - \tan^{-1}(1.7e^{(E_{mn}-E_c)/kT})\right]. \quad \text{(A8)}$$

Generally speaking, $(E_{mn}-E_v)/kT$, $(E_c-E_{mn})/kT \gg 1$, so that the contents of the square brackets evaluate to approximately $\frac{1}{2}\pi$, hence (A8) reduces to

$$D = 1.2kT\nu e^{(E_{mn}-E_c)/kT} \quad \text{(A9)}$$

or, by using (8),

$$D = 1.2\beta(E_c - E_{mn})/T. \quad \text{(A10)}$$

*Supported in part by National Research Council and Defense Research Board of Canada.

†Now with Uniroyal Research Center, Guelph, Ontario, Canada.

[1]J. J. Randall and M. H. F. Wilkens, Proc. Roy. Soc. A184, 366 (1945); A184, 390 (1945).
[2]K. H. Nicholas and J. Woods, Brit. J. Appl. Phys. 15, 783 (1964).
[3]G. A. Dussel and R. H. Bube, Phys. Rev. 155, 764 (1967).
[4]R. Chen, J. Appl. Phys. 40, 570 (1969).
[5]I. J. Saunders, J. Phys. 2, 2181 (1969).
[6]P. S. Pickard and M. V. Davis, J. Appl. Phys. 41, 2636 (1970).
[7]P. Kelly and P. Braunlich, Phys. Rev. B 1, 1587 (1970).
[8]J. G. Simmons and G. W. Taylor, Phys. Rev. B 4, 502 (1971).
[9]J. G. Simmons and G. W. Taylor, Phys. Rev. B 5, 1619 (1972).
[10]J. G. Simmons and M. C. Tam, preceding paper, Phys. Rev. B 7, 3706 (1973).
[11]J. G. Simmons and G. W. Taylor, Phys. Rev. B (to be published).
[12]J. G. Simmons and G. W. Taylor, Phys. Rev. B (to be published).
[13]J. G. Simmons and G. S. Nadkarni, Phys. Rev. B (to be published).

PHYSICAL REVIEW B VOLUME 7, NUMBER 8 15 APRIL 1973

Isothermal-Dielectric-Relaxation Currents in Thin-Film Al-CeF_3-Al Samples*

G. S. Nadkarni† and J. G. Simmons
Electrical Engineering Department, University of Toronto, Toronto, Canada
(Received 2 June 1972)

A new technique based on isothermal-dielectric-relaxation currents (IDRC) had been successfully used to study the defect properties of thin-film Al-CeF_3-Al samples. The IDRC technique consists of applying a step voltage to the sample to induce a non-steady state and then measuring the non-steady-state current as a function of time as the system decays to the steady state. It is found that at low temperatures ($T < 250$ °K), the displacement charge Q_d circulating the external circuit is associated with the geometrical capacitance. Thus, it is inversely proportional to the thickness of the sample and linearly dependent on the voltage. At higher temperatures ($T > 280$ °K) a pronounced dielectric-relaxation current flows through the insulator. The displacement charge Q_r associated with the relaxation current is found to be 20–40 times the magnitude of Q_d and *independent* of the thickness of the insulator at low voltages, indicating the existence of Schottky barriers at the electrode insulator and, thus, that the conduction process is electrode limited. At higher voltages $V \gtrsim 4$ V, Q_r saturates showing that the conduction process is bulk limited. From the Q_r-V characteristic, the trapping density is found to be 6×10^{19} cm^{-3}. The It-$\log_{10}t$ characteristic is shown to manifest a pronounced peak. From this characteristic, it is determined that the occupied trap levels are contained in a band of energy of width approximately 0.02 eV, which is centered about an energy 0.63 ± 0.03 eV below the bottom of the conduction band. The results are shown to be consistent with IDRC theory and previous stimulated-dielectric-relaxation-current studies on the same samples.

I. INTRODUCTION

In recent papers it was shown, on theoretical grounds, that Schottky barriers can exist at the metal-insulator interface of metal-insulator-metal (MIM) systems when the insulator is defect in nature.[1–3] ac and dc measurements[4–8] on MoO_3, SiO, and CeF_3 films have confirmed the existence of these barriers. Stimulated-dielectric-relaxation-current[7,8] (SDRC) measurements on a wide variety of materials (MoO_3, SiO, CeF_3, $BaTiO_3$, Al_2O_3, and many semiconducting glasses) have also shown Schottky barriers to exist at the electrode-insulator/semiconductor interfaces.